2D CAVITY MODELING USING METHOD OF MOMENTS AND ITERATIVE SOLVERS

C.-F. Wang and Y.-B. Gan

Temasek Laboratories
National University of Singapore
10 Kent Ridge Crescent, Singapore 119260

Abstract—The method of moments (MoM) and the electric field integral equations (EFIEs), for both parallel and perpendicular polarization were applied to simulate scattering from 2D cavity structures. This code employed several matrix equation solvers, such as the LU decomposition, conjugate gradient (CG) method, bi-conjugate gradient (BCG) method, generalized conjugate residual (GCR) method, and generalized minimal residual (GMRES) method. The simulated results can be used for future reference and benchmarking. A comparison on the convergence behavior of the CG, BCG, GCR, and GMRES methods was made for the benchmark geometry, such as offset bend cavity, rectangular waveguide with hub, double-bend S-shaped cavity, etc. Some comments on the performance of the various iterative solvers will be highlighted.

1 Introduction

2 Formulation

3 Numerical Results

4 Conclusion

Acknowledgment

References

1. INTRODUCTION

Air intake system is a significant contributor to the overall electromagnetic (EM) signature of real target. It is therefore necessary to provide an accurate characterization of its effect and scattering

contribution. This is a rather challenging task, due to the intricate details associated with the engine blade configuration, the engine's large electrical size, and the complex, non-canonical shape of practical inlet. Several approaches have been studied for this important and challenging task. These include the shooting-and-bouncing-ray (SBR) method [1–3], the Gaussian beam shooting method [4–6], the generalized ray expansion (GRE) method [7], the iterative physical optics (IPO) method [8], and the field iterative method (FIM) [9]. When a cavity is small, numerical techniques such as the variational equation based method [10]-[11] and the finite element method (FEM) [12, 13] can be applied for the calculation of scattering pattern. Recently, a very efficient FEM based numerical technique has been proposed for the analysis of electromagnetic scattering from large, deep, and arbitrarily-shaped open cavity in [14]. In addition to aforementioned techniques, a variety of hybrid techniques combining a high-frequency and a numerical method have also been proposed to solve the cavity scattering problems [15–18]. These hybrid techniques are intended to reduce the size of the computational domain for the numerical method and thus increase the efficiency and capability of their solutions.

In order to obtain a deeper understanding on the scattering from cavity, a 2D cavity modeling code was implemented using the method of moments (MoM) and the electric field integral equations (EFIEs) for both parallel and perpendicular polarization. In fact, the 2D cavity modeling is important for some typical structures, as we can obtain the 3D scattering pattern from 2D results to assist in understanding the effect of structure profile. In this paper, we will put our emphasis on in-depth understanding of the mathematical behaviour of resultant linear system for cavity problem. This code employed several matrix equation solvers, such as the LU decomposition (LUD), conjugate gradient (CG) method [13, 19], bi-conjugate gradient (BCG) method [19–21], generalized conjugate residual (GCR) method [19, 22], and generalized minimal residual (GMRES) method [23]. The code has been verified and is able to provide reasonable results for several 2D reference geometry, such as the offset bend cavity, rectangular waveguide with hub, double-bend S-shaped cavity, etc. These results can be used for future reference and benchmarking. A comparison on the convergence behavior of the CG, BCG, GCR, and GMRES methods was made for the benchmark geometry that we have computed.
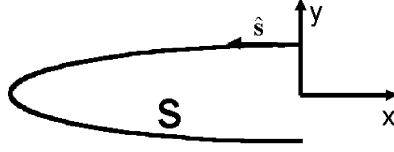
Figure 1. The geometry of a general cavity structure.

2. FORMULATION

Consider an arbitrarily-shaped 2D cavity structure (as shown in Fig. 1) illuminated by an incident field $\mathbf{E}^{inc}(\boldsymbol{\rho})$, the electric field integral equation (EFIE) for parallel polarization (TMz) is given by [24]

$$-E^{inc}(\boldsymbol{\rho}) = -\frac{\omega\mu}{4} \int_S J_z(\boldsymbol{\rho}') H_0^{(2)}(k|\boldsymbol{\rho} - \boldsymbol{\rho}'|) ds' \qquad \text{on } S \qquad (1)$$

where μ is the permeability and k is the wavenumber of free space, S denotes the conducting surface of the cavity, and $H_0^{(2)}$ is the Hankel function of second kind and zero order. The EFIE for perpendicular polarization (TEz) is given by [24]

$$-\mathbf{E}^{inc}(\boldsymbol{\rho})\cdot\hat{\mathbf{s}} = [-j\omega\mathbf{A}(\boldsymbol{\rho}) - \nabla\Phi(\boldsymbol{\rho})]\cdot\hat{\mathbf{s}} \qquad \text{on } S \qquad (2)$$

The vector and scalar potentials in (2) are given by

$$\mathbf{A}(\boldsymbol{\rho}) = \frac{\mu}{4j} \int_S \mathbf{J}(\boldsymbol{\rho}') \, H_0^{(2)}(k|\boldsymbol{\rho} - \boldsymbol{\rho}'|) ds' \qquad (3)$$

and

$$\Phi(\boldsymbol{\rho}) = \frac{1}{4j\varepsilon} \int_S \rho(\boldsymbol{\rho}') \, H_0^{(2)}(k|\boldsymbol{\rho} - \boldsymbol{\rho}'|) ds' \qquad (4)$$

respectively, where $\mathbf{J}(\boldsymbol{\rho}) = \hat{\mathbf{s}}(\boldsymbol{\rho})J(\boldsymbol{\rho})$ is the s-directed current density and ρ is the surface charge density which is related to the current through the equation of continuity,

$$\rho(\boldsymbol{\rho}) = \frac{j}{\omega}\nabla_s \cdot \mathbf{J}(\boldsymbol{\rho}) \qquad (5)$$

Equation (1) can be discretized into a linear system using the MoM with any basis and testing functions, such as pulse and triangle functions. Equation (2) is slightly more complicated than equation (1) because of the differential operators appearing in the equation. In contrast to equation (1), equation (2) involves both vector and scalar
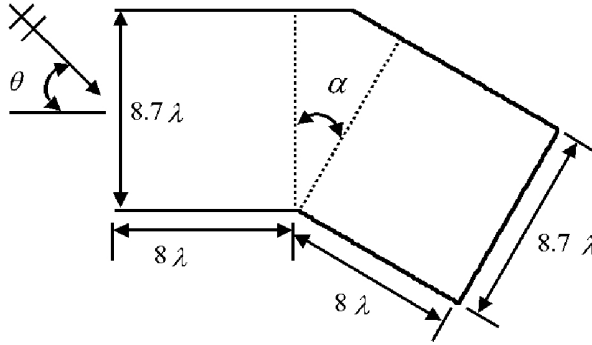
Figure 2. The geometry of a 2D bent cavity structure.

potentials, corresponding to current and charge, respectively. It is advisable to use basis and testing functions having additional degrees of differentiability to compensate for the additional derivatives present in equation (2). The triangle basis functions with pulse testing functions together provide two degrees of differentiability, beyond that of the pulse/Dirac delta combination. In order to take advantage of this fact, the triangle basis functions are chosen for expressing the current distribution on the surface of cavity. More discussion and details on the discretization of the equation (2) can be found in [24–26]. The MoM equation for both EFIEs can expressed as

$$ZI = V \tag{6}$$

The matrix equation (6) can be solved using matrix equation solvers, such as the LU decomposition, the CG, BCG, GCR, and GMRES methods [13, 19–23].

3. NUMERICAL RESULTS

The first problem that we have investigated is the scattering from a 2D bent cavity structure shown in Fig. 2. Figs. 3–5 show the backscatter patterns for perpendicular polarization with $\alpha = 15°$, $30°$, and $45°$. All the simulated results agree well with the results obtained using FEM [14] or BIM/Mode approach [27].

The second problem that we have investigated is an offset bend cavity structure, as shown in Fig. 6. The backscatter patterns of the offset bend cavity at 10 GHz for both parallel and perpendicular polarization are given in Figs. 7 and 8. From these two figures, we
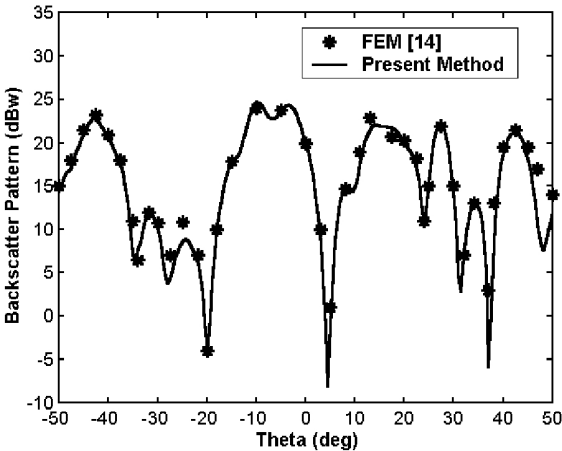
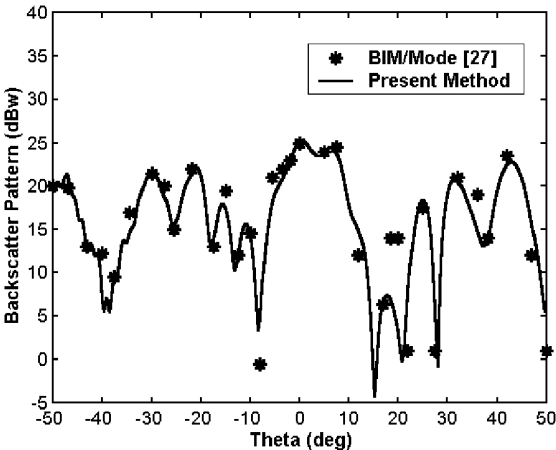**Figure 3.** The backscatter patterns of the 2D bent cavity structure with $\alpha = 15°$: parallel polarization.

Figure 4. The backscatter patterns of the 2D bent cavity structure with $\alpha = 30°$: parallel polarization.
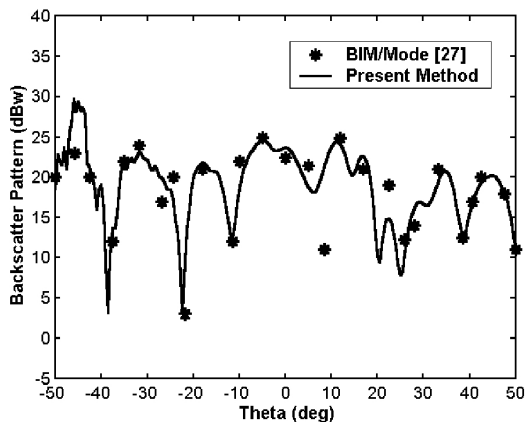
Figure 5. The backscatter patterns of the 2D bent cavity structure with $\alpha = 45°$: parallel polarization.
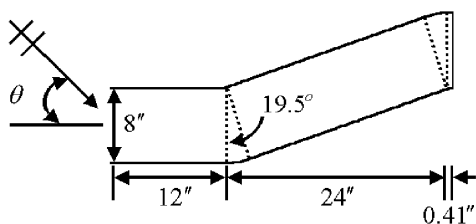

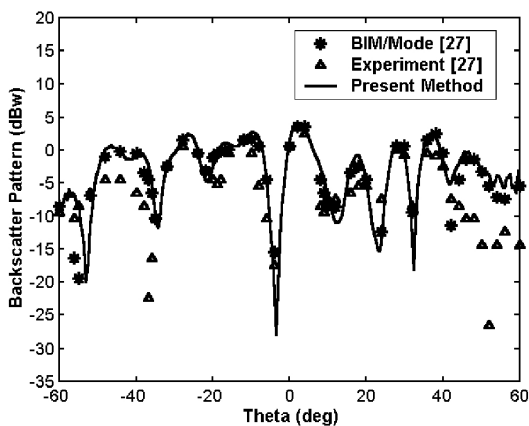**Figure 6.** The geometry of a offset bend cavity structure.

Figure 7. The backscatter patterns of the offset bend cavity structure: parallel polarization.
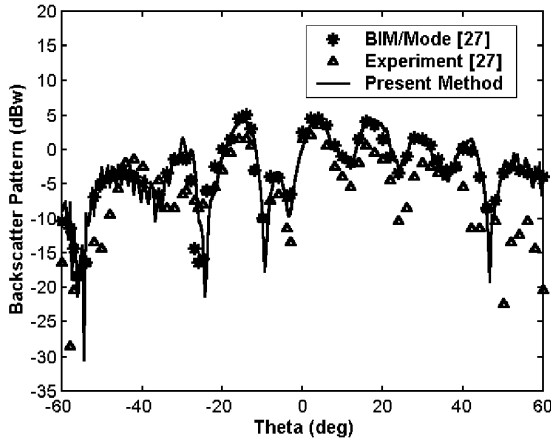
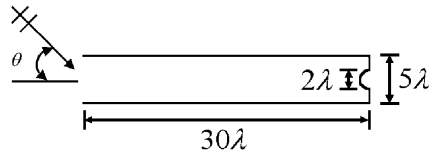**Figure 8.** The backscatter patterns of the offset bend cavity structure: perpendicular polarization.

Figure 9. The geometry of a waveguide cavity with semicircular hub at the termination.
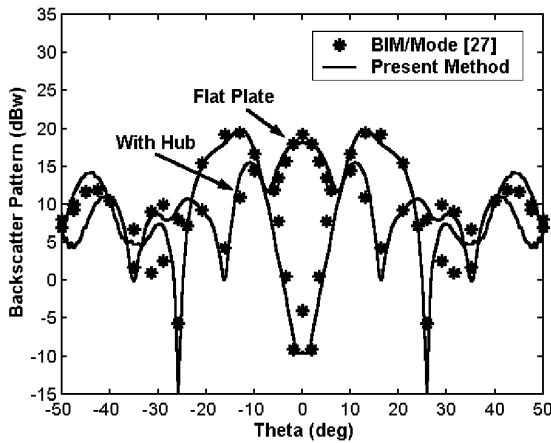

Figure 10. The backscatter patterns of the waveguide cavity with semicircular hub at the termination: parallel polarization.
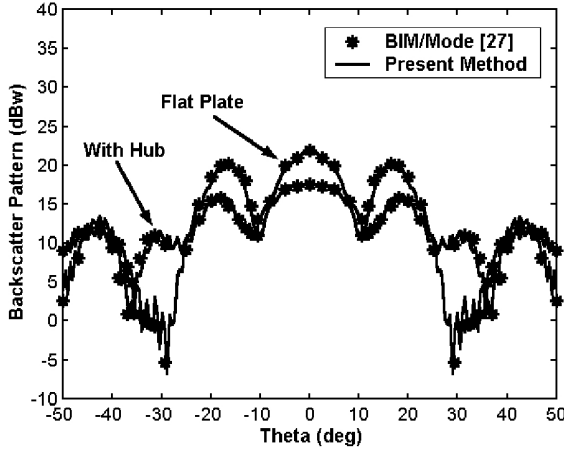
Figure 11. The backscatter patterns of the waveguide cavity with semicircular hub at the termination: perpendicular polarization.
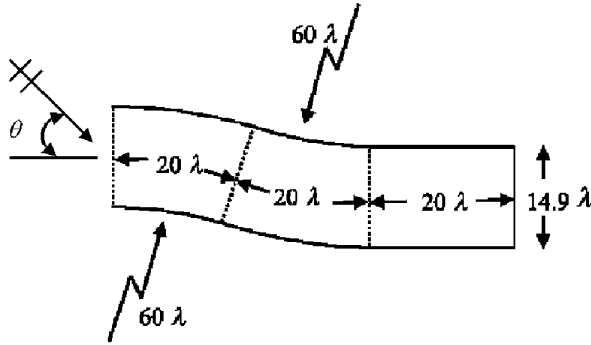

Figure 12. The geometry of a 2D double-bend S-shaped cavity.

observed that the results obtained using the present method are in good agreement with the results obtained using measurement and BIM/Mode approaches [27].

The third problem was investigated was the scattering from a waveguide cavity with semicircular hub at the termination. The geometry is shown in Fig. 9. Figs. 10 and 11 show the backscatter patterns for both parallel and perpendicular polarization. The results obtained using the present method and the BIM/Mode approach [27] are in good agreement. Figs. 10 and 11 also indicated that the termination has a very significant effect on the backscatter pattern
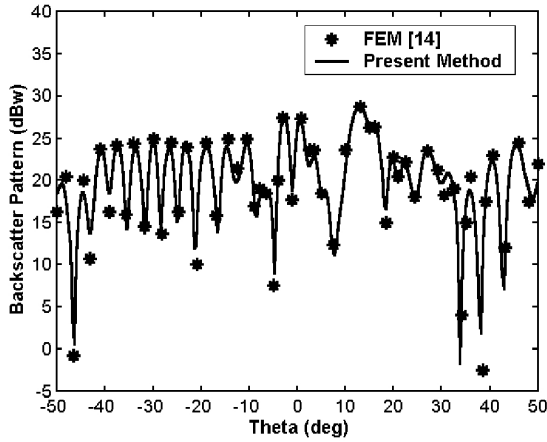
Figure 13. The backscatter patterns of the 2D double-bend S-shaped cavity: perpendicular polarization.
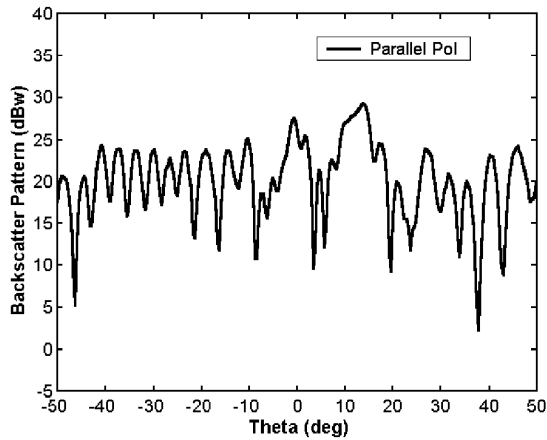

Figure 14. The backscatter patterns of the 2D double-bend S-shaped cavity: parallel polarization.

near normal incidence and that the effect is highly dependent on the polarization.

The more complex problem investigated is the scattering from a 2D double-bend S-shaped cavity. The geometry is given in Fig. 12. The backscatter pattern for perpendicular polarization is shown in Fig. 13. The two scattering patterns agree well.

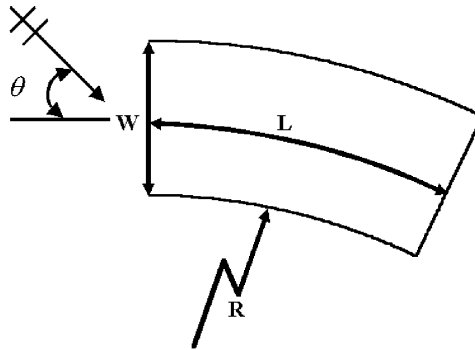All the test cases mentioned above illustrated that the code

Figure 15. The geometry of an open-ended annular waveguide with a short circuit termination.
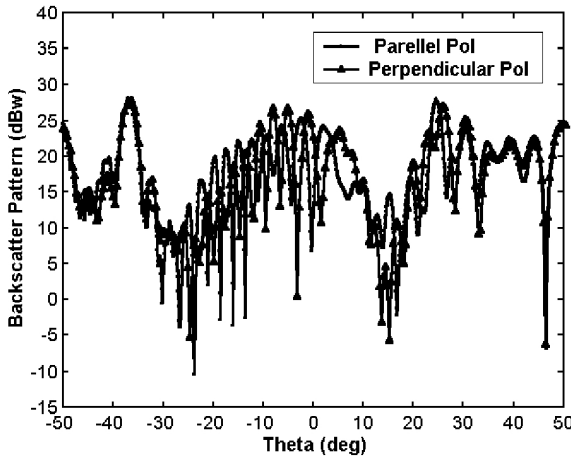

Figure 16. The backscatter patterns of the open-ended annular waveguide with a short circuit termination: $W = 14.9\lambda$, $L = 30\lambda$, $R = 60\lambda$.

developed by us is accurate and reliable. More cavity structures were simulated for benchmarking purpose. Fig. 14 shows the backscatter pattern of the 2D double-bend S-shaped cavity for parallel polarization.

Fig. 15 shows an open-ended annular waveguide with a short circuit termination. The backscatter patterns of the open-ended annular waveguide with different dimensions have been simulated using the present method for both parallel and perpendicular polarization. Fig. 16 shows the backscatter patterns of the open-ended annular
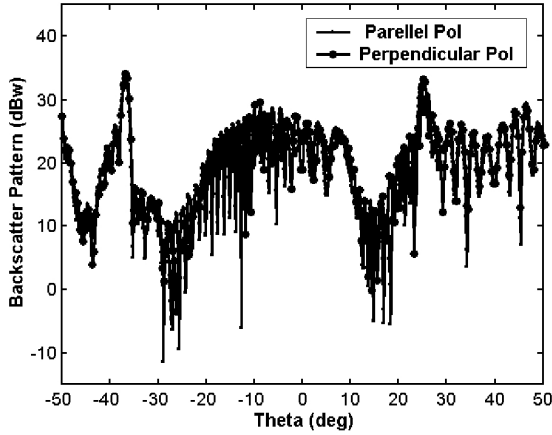
Figure 17. The backscatter patterns of the open-ended annular waveguide with a short circuit termination: $W = 29.8\lambda$, $L = 60\lambda$, $R = 120\lambda$.
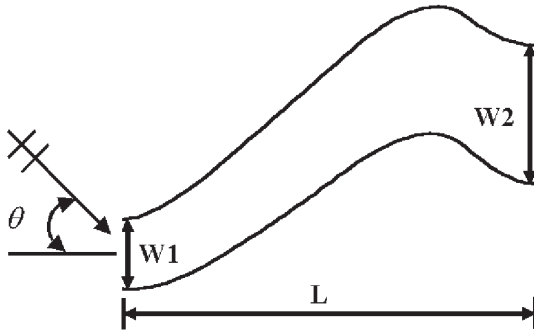

Figure 18. The geometry of an aerodynamic cavity structure: $W_1 = 0.5\,\text{m}$, $W_2 = 1.0\,\text{m}$, $L = 3.0\,\text{m}$.

waveguide with dimensions: $W = 14.9\lambda$, $L = 30\lambda$, and $R = 60\lambda$. Fig. 17 shows the backscatter patterns of the open-ended annular waveguide with dimensions: $W = 29.8\lambda$, $L = 60\lambda$, and $R = 120\lambda$. From Figs. 16 and 17, it is observed that the backscatter patterns are slightly dependent on the polarization. The reason is that the aperture size of the cavity is electrically large.

The last problem investigated is the scattering from an aerodynamic cavity as shown in Fig. 18. The dimensions of the aerodynamic cavity are $W_1 = 0.5$ m, $W_2 = 1.0\,\text{m}$, and $L = 3.0\,\text{m}$.
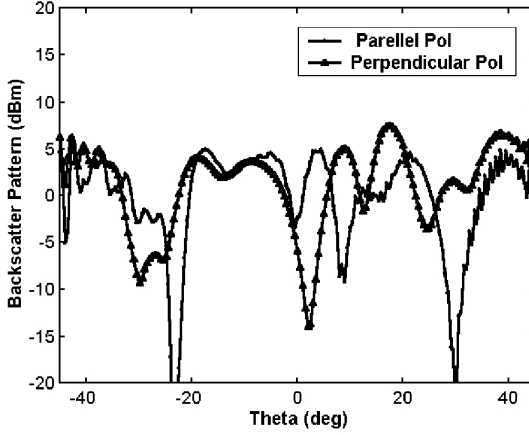
Figure 19. The backscatter patterns of the aerodynamic cavity structure.
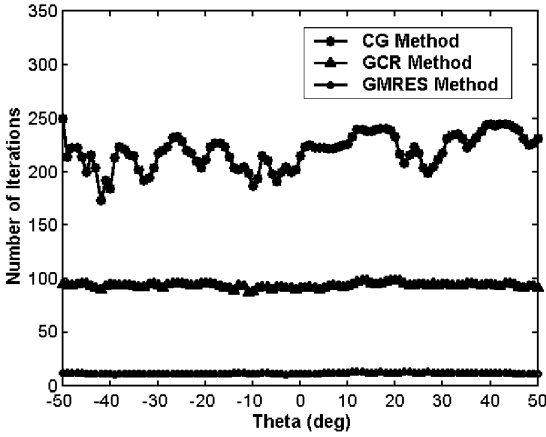

Figure 20. The convergence behaviour of iterative solvers for the 2D bent cavity structure: parallel polarization.

The backscatter patterns of the aerodynamic cavity at $3.0\,\mathrm{GHz}$ are given in Fig. 19.

In order to obtain an in-depth understanding on the mathematical behaviour of the resultant linear system for cavity problems, the code was implemented using five matrix solvers: LUD, CG, BCG, GCR, and GMRES methods. Of the four iterative solvers (CG, BCG, GCR, GMRES), the BCG method is not stable for cavity modeling.
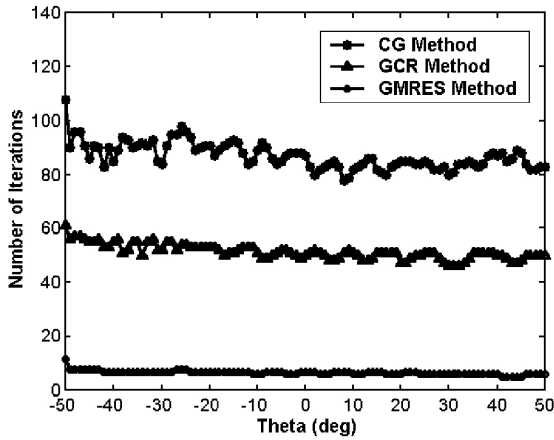
Figure 21. The convergence behaviour of iterative solvers for the 2D bent cavity structure: perpendicular polarization.
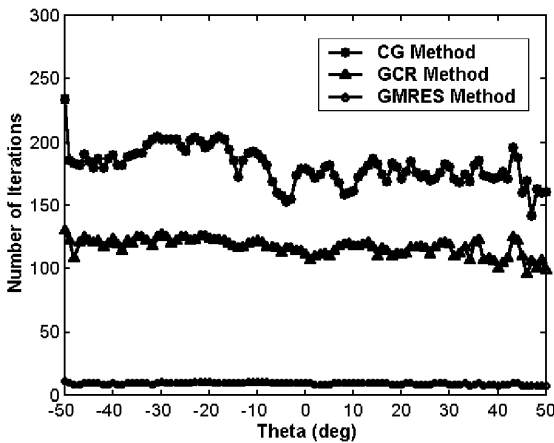

Figure 22. The convergence behaviour of iterative solvers for the offset bend cavity structure: parallel polarization.

Figs. 20 and 21 show the convergence behaviour of CG, GCR and GMRES methods for simulating the 2D bent cavity for both parallel and perpendicular polarization. It is observed that the GCR and GMRES methods converge much faster than the CG method.

Figs. 22 and 23 show the convergence behaviour of CG, GCR and GMRES iterative solvers for simulating the offset bend cavity for both parallel and perpendicular polarization. Figs. 22 and 23 show that
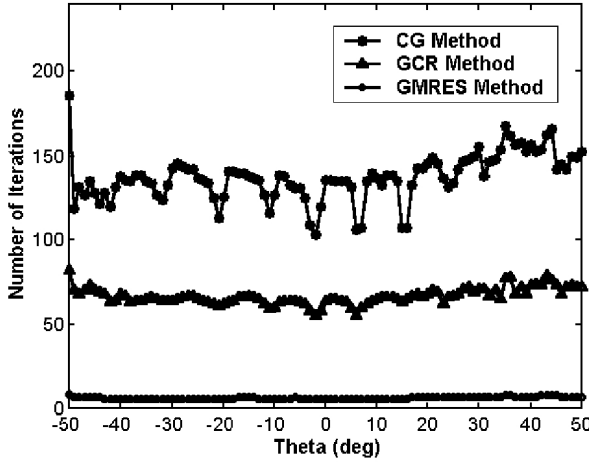
Figure 23. The convergence behaviour of iterative solvers for the offset bend cavity structure: perpendicular polarization.

the GCR and GMRES methods converge much faster than the CG method, too.

The convergence behaviour of CG, GCR and GMRES methods for simulating the 2D double-bend S-shaped for both parallel and perpendicular polarization is shown in Figs. 24 and 25, which show that the GCR and GMRES methods converge much faster than the CG method.

The convergence behaviour of CG, GCR and GMRES methods have been tested by simulating the other three benchmark cavities for both parallel and perpendicular polarization. The results shown in Figs. 26 and 29 show that the GCR and GMRES methods converge much faster than the CG method, as well.

From the simulation of the scattering from all six typical cavities considered in this paper, for both parallel and perpendicular polarization, we observed that:

a. The BCG method is not suitable for use in 2D cavity modeling, while the CG, GCR, and GMRES methods are acceptable.

b. The convergence behaviour of GCR and GMRES methods is much better than that of the CG method. The GCR and GMRES methods incur more memory due to the requirement of the auxiliary arrays. This is still affordable in MoM solver, since the sizes of the auxiliary arrays are much smaller compared to the size of the matrix. The CG method does not incur more memory.
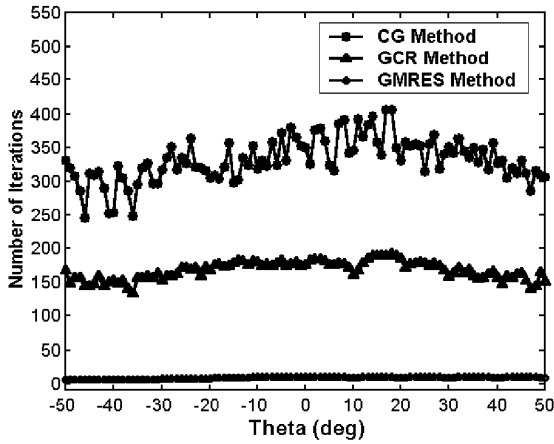
Figure 24. The convergence behaviour of iterative solvers for the 2D double-bend S-shaped cavity structure: parallel polarization.
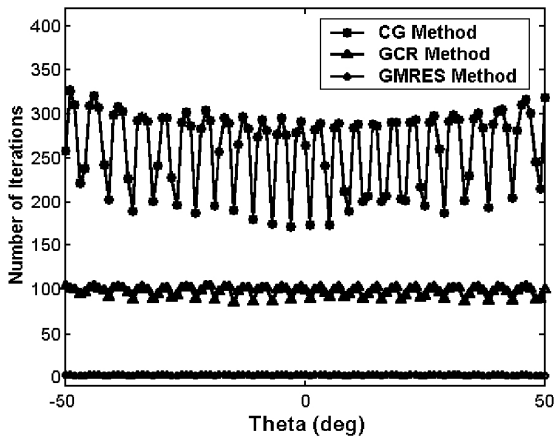

Figure 25. The convergence behaviour of iterative solvers for the 2D double-bend S-shaped cavity structure: perpendicular polarization.

Hence, it is a good candidate for fast algorithm on 2D cavity modeling.

c. The iterative solvers need to be preconditioned, to improve their robustness for complex cavity structures, especially for deep cavity structures.
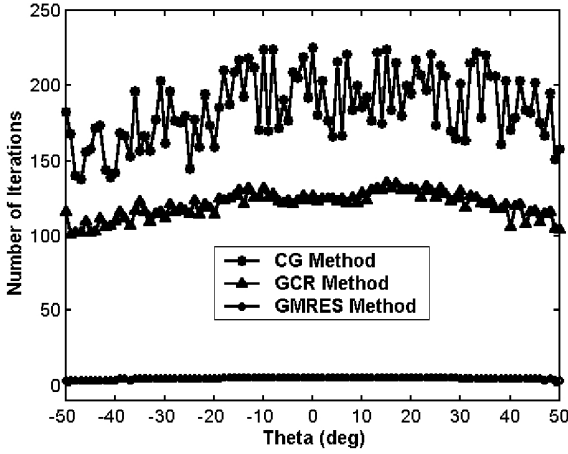
Figure 26. The convergence behaviour of iterative solvers for the annular waveguide with a short circuit termination: parallel polarization.

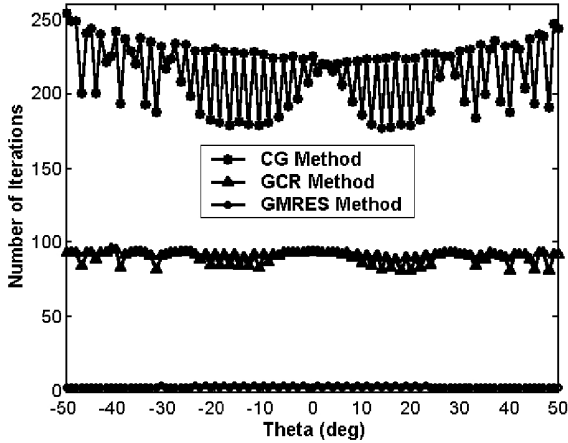**Figure 27.** The convergence behaviour of iterative solvers for the annular waveguide with a short circuit termination: perpendicular polarization.

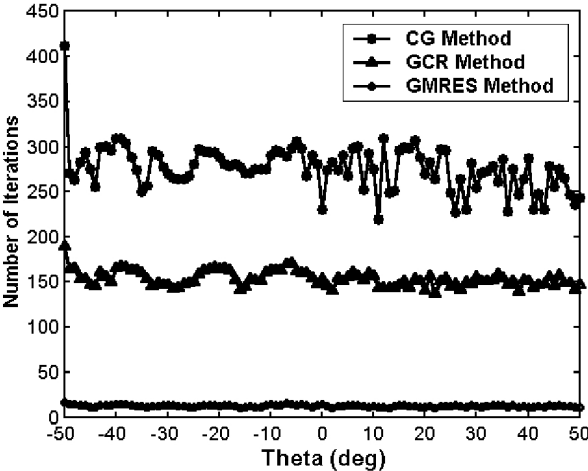**Figure 28.** The convergence behaviour of iterative solvers for the aerodynamic cavity structure: parallel polarization.
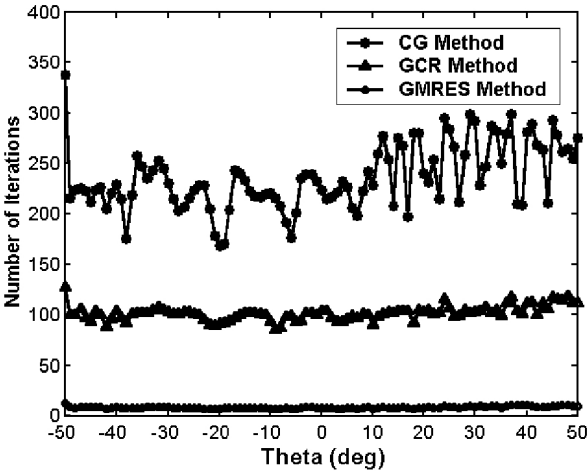

Figure 29. The convergence behaviour of iterative solvers for the aerodynamic cavity structure:perpendicular polarization.

4. CONCLUSION

The method of moments (MoM) and the electric field integral equations (EFIEs), for both parallel and perpendicular polarization were applied to simulate the scattering from 2D cavity structures. This code employed several matrix equation solvers, such as the LUD, CG, BCG, GCR, and GMRES methods. The simulated results can be used for future reference and benchmarking. A comparison on the convergence behavior of the CG, BCG, GCR, and GMRES methods was made for the benchmark geometry, such as offset bend cavity, rectangular waveguide with hub, double-bend S-shaped cavity, etc. The comments on the iterative solvers obtained in this paper can be used as a guide to cavity modeling.

ACKNOWLEDGMENT

REFERENCES

1. Ling, H., R. Chou, and S. W. Lee, "Rays versus modes: pictorial display of energy flow in an open-ended waveguide," *IEEE Trans. Antennas Propagat.*, Vol. 35, No. 5, 605–607, May 1987.

2. Ling, H., R. Chou, and S. W. Lee, "Shooting and bouncing rays: calculation RCS of an arbitrarily shaped cavity," *IEEE Trans. Antennas Propagat.*, Vol. 37, No. 2, 194–205, Feb. 1989.

3. Ling, H., R. Chou, and S. W. Lee, "High-frequency RCS of open cavities with rectangular and circular cross sections," *IEEE Trans. Antennas Propagat.*, Vol. 37, No. 5, 648–654, May 1989.

4. Pathak, P. H. and R. J. Burkholder, "Modal, ray and beam techniques for analyzing the EM scattering by open-ended waveguide cavities," *IEEE Trans. Antennas Propagat.*, Vol. 37, No. 5, 635–647, May 1989.

5. Pathak, P. H. and R. J. Burkholder, "High-frequency electromagnetic scattering by open-ended waveguide cavities," *Radio Science*, Vol. 26, 211–218, Jan.–Feb. 1991.

6. Burkholder, R. J., R. C. Chou, and P. H. Pathak, "Analysis of EM penetration scattering by electrically large open waveguide cavities using Gaussian beam shooting," *Proc. IEEE*, Vol. 79, 1401–1412, Oct. 1991.

7. Pino, A. G., F. Obelleiro, and J. L. Rodriguez, "Scattering from conducting open cavities by generalized ray expansion (GRE)," *IEEE Trans. Antennas Propagat.*, Vol. 41, No. 7, 989–992, July 1993.

8. Obelleiro-Basteiro, F., J. L. Rodriguez, and R. J. Burkholder, "An iterative physical optics approach for analyzing the electromagnetic scattering by large open-ended cavities," *IEEE Trans. Antennas Propagat.*, Vol. 43, No. 4, 356–361, April 1995.

9. Reuster, D. D. and G. A. Thiele, "A field iterative method for computing the scattering electric fields at the apertures of large perfect conducting cavities," *IEEE Trans. Antennas Propagat.*, Vol. 43, No. 3, 286–290, March 1995.

10. Jeng, S. K., "Scattering from a cavity-backed slit in a ground plane-TE case," *IEEE Trans. Antennas Propagat.*, Vol. 38, No. 10, 1523–1529, Oct. 1990.

11. Jeng, S. K. and S. T. Tzeng, "Scattering from a cavity-backed slit in a ground plane-TM case," *IEEE Trans. Antennas Propagat.*, Vol. 39, No. 5, 661–663, May 1991.

12. Jin, J. M. and J. L. Volakis, "A finite element-boundary integral formulation for scattering by three-dimensional cavity-backed aperture," *IEEE Trans. Antennas Propagat.*, Vol. 39, No. 1, 97–104, Jan. 1991.

13. Jin, J. M., *The Finite Element Method in Electromagnetics*, Wiley, New York, 1993.

14. Jin, J. M., "Electromagnetic scattering from large, deep, and arbitrarily-shaped open cavities," *Electromagn.*, Vol. 18, No. 1, 3–34, 1998.

15. Lee, R. and T. T. Chia, "Analysis of electromagnetic scattering from a cavity with a complex termination by means of a hybrid ray-FDTD method," *IEEE Trans. Antennas Propagat.*, Vol. 41, No. 11, 1560–1569, Nov. 1993.

16. Ross, D. C., J. L. Volakis, and H. T. Anastassiu, "Hybrid finite element-modal analysis of jet engine inlet scattering," *IEEE Trans. Antennas Propagat.*, Vol. 43, No. 3, 277–285, March 1995.

17. Jin, J. M., S. Ni, and S. W. Lee, "Hybridization of SBR and FEM for scattering by large bodies with cracks and cavities," *IEEE Trans. Antennas Propagat.*, Vol. 43, No. 10, 1130–1139, Oct. 1995.

18. Chia, T. T., R. J. Burkholder, and R. Lee, "The application of FDTD in hybrid methods for cavity scattering analysis," *IEEE Trans. Antennas Propagat.*, Vol. 43, No. 10, 1082–1090, Oct. 1995.

19. Saad, Y., *Iterative Methods for Sparse Linear Systems*, PWS, New

York, 1995.

20. Lanczos, C., "Solution of systems of linear equations by minimized iterations," *J. Res. Nat. Bur. Standards*, Vol. 49, 33–53, 1952.

21. Fletcher, R., "Conjugate gradient methods for indefinite systems," *Lecture Notes in Math.*, 506, Berlin, Heidelberg, Springer-Verlag, New York, 73–89, 1976.

22. Eisenstat, S. C., H. C. Elman, and M. H. Schultz, "Variational iterative methods for non-symmetric systems of linear equations," *SIAM J. Numer. Anal.*, Vol. 20, 345–357, 1983.

23. Saad, Y. and M. H. Schultz, "GMRES: A generalized minimal residual algorithm for solving nonsymmetric linear systems," *SIAM J. Sci. Statist. Comput.*, Vol. 7, 856–869, July 1986.

24. Glisson, A. W. and D. R. Wilton, "Simple and efficient numerical methods for problems of electromagnetic radiation and scattering from surfaces," *IEEE Trans. Antennas Propagat.*, Vol. 28, No. 5, 593–603, Sept. 1980.

25. Wilton, D. R. and S. Govind, "Incorporation of edge conditions in moment method solution," *IEEE Trans. Antennas Propagat.*, Vol. 5, No. 6, 845–850, Nov. 1977.

26. Harrington, R. F., *Field Computation by Moment Methods*, Krieger, FL, 1982.

27. Ling, H., "RCS of waveguide cavities: a hybrid boundary-integral/modal approach," *IEEE Trans. Antennas Propagat.*, Vol. 38, No. 9, 1413–1420, Sept. 1990.